Electrolytic Conductivity and Glass Transition Temperature as Functions of Salt Content, Solvent Composition, or Temperature for $LiPF_6$ in Propylene Carbonate + Diethyl Carbonate

Michael S. Ding*

Army Research Laboratory, 2800 Powder Mill Road, Adelphi, Maryland 20783

The electrolyte system of $LiPF_6$ in propylene carbonate (PC) + diethyl carbonate (DEC) was measured for its electrolytic conductivity κ at salt molalities m, solvent compositions w, and temperatures θ in the ranges of (0.2, 2.4) mol kg^{-1}, (0, 0.7) mass fraction of DEC, and (−80, 60) °C, respectively, and for its glass transition temperatures T_g in the same ranges of m and w. The measured $\kappa-(m, w)$ data at different θ were further fitted with an extended version of the Casteel−Amis equation in order to observe the change of κ with simultaneous changes of m and w and with θ. The κ surfaces according to these fitted equations all assumed a "dome" shape as a result of κ peaking in both m and w. Furthermore, as θ lowered, these domes fell in height and shifted in the direction of low m and high w, the direction of lower viscosity η. The T_g was found to rise with m and fall with w, indicating a concurrent change in the η of the solution. The measured $\kappa-T$ data were fitted with the Vogel−Fulcher−Tammann equation for an evaluation of the vanishing mobility temperature T_0 and the apparent activation energy E_a for the electrolytes, both shown to form simple surfaces in the mw-coordinates slanting up in the direction of higher η. Furthermore, when compared to the surface of T_g, that of T_0 was oriented similarly but lower in value by more than 10 K.

Introduction

Electrolytes formed between an organic carbonate solvent or mixture and one of a few lithium salts (particularly $LiPF_6$ and $LiBF_4$) have long been established as the most suitable electrolytes for lithium-ion batteries.[1,2] This suitability comes as a result of the high electrochemical stability of the electrolytes which enables the use of highly energetic lithium−metal oxide cell chemistry, their moderately high electrolytic conductivity which, by reducing the electrolyte resistance and polarization, gives rise to the high power capability of the batteries in which they serve as the electrolyte, and the ease with which their physical properties can be tailored to particular needs through adjustment of their composition. Common carbonate solvents for this use include ethylene carbonate (EC), propylene carbonate (PC), dimethyl carbonate (DMC), ethyl methyl carbonate (EMC), and diethyl carbonate (DEC), of which many components or mixtures have been systematically studied for their dielectric constant (ϵ),[3−11] viscosity (η),[4−10,12−15] and phase equilibrium,[16−19] in regard to their battery application. In the same regard, electrolytic conductivities (κ) of many of the solutions have been measured as functions of salt content (denoted here as molality m), solvent composition (mass fraction w), and temperature (θ/°C or T/K).[6−10,20−30] But so far, these κ measurements have largely been restricted to those where the dependency of κ on m is studied separately from that on w, with only a few exceptions. Two recent examples for the exception are the studies on electrolyte systems $LiPF_6(m) + (1 - w)EC + wEMC$[21] and $LiPF_6(m) + (1 - w)EC_{0.3}PC_{0.3}EMC_{0.4} + w$TFP,[6] where TFP stands for tris-(2,2,2-trifluoroethyl) phosphate, for which κ was measured in the ranges of m of (0.4, 1.6) mol kg^{-1}, w of (0.23, 0.54) for the former and (0, 0.4) for the latter, and θ of (−40, 60) °C. In these studies, the measured $\kappa-(m, w, \theta)$ data were fitted successfully with trivariate polynomial functions $\kappa = f(m,w,\theta)$, which by presenting κ as 3D surfaces in mw-coordinates greatly helped in the elucidation of the pattern and the mechanisms of the change of κ with simultaneous changes of m and w and thereby in the optimization of the electrolytes through proper formulation. However, for $\kappa-(m, w, \theta)$ data with a more extended range of m, the same trivariate polynomial fitting function was inadequate because of the inadequacy of univariate polynomial functions $\kappa = f(m)$ in fitting $\kappa-m$ data with an extended m-range. The latter kind of $\kappa-m$ data is known to be best fitted with the four-parameter, univariate Casteel−Amis equation;[31] however, the equation has yet to be modified in order to extend its use to fitting the $\kappa-(m, w)$ data for the purpose of presenting and observing the change of κ with simultaneous changes of m and w.

The aim of this paper is therefore first and mainly to present a relatively complete set of $\kappa-(m, w, \theta)$ data in numerical form for the electrolyte $LiPF_6(m) + (1 - w)$PC + wDEC in the ranges of m, w, and θ of (0.2, 2.4) mol kg^{-1}, (0, 0.7) mass fraction, and (−80, 60) °C, respectively. This is to complement another paper on the same set of measurements in which space has only been given to the interpretation and application of the results but not to the tabulation of the numerical values.[32] It is second to describe an extended version of the Casteel−Amis equation for its use in fitting the $\kappa-(m, w)$ data and to demonstrate the high degree to which the extended function can be satisfactorily fitted to the experimental data and the fitted functions plotted to reveal the changes of κ with m and w at different θ. It is third to provide another set of numerical data of glass transition temperature (T_g) for the electrolyte, insofar as could be experimentally determined, in the same

* E-mail: mding@arl.army.mil.

10.1021/je020219o CCC: $25.00
Published on Web 04/12/2003

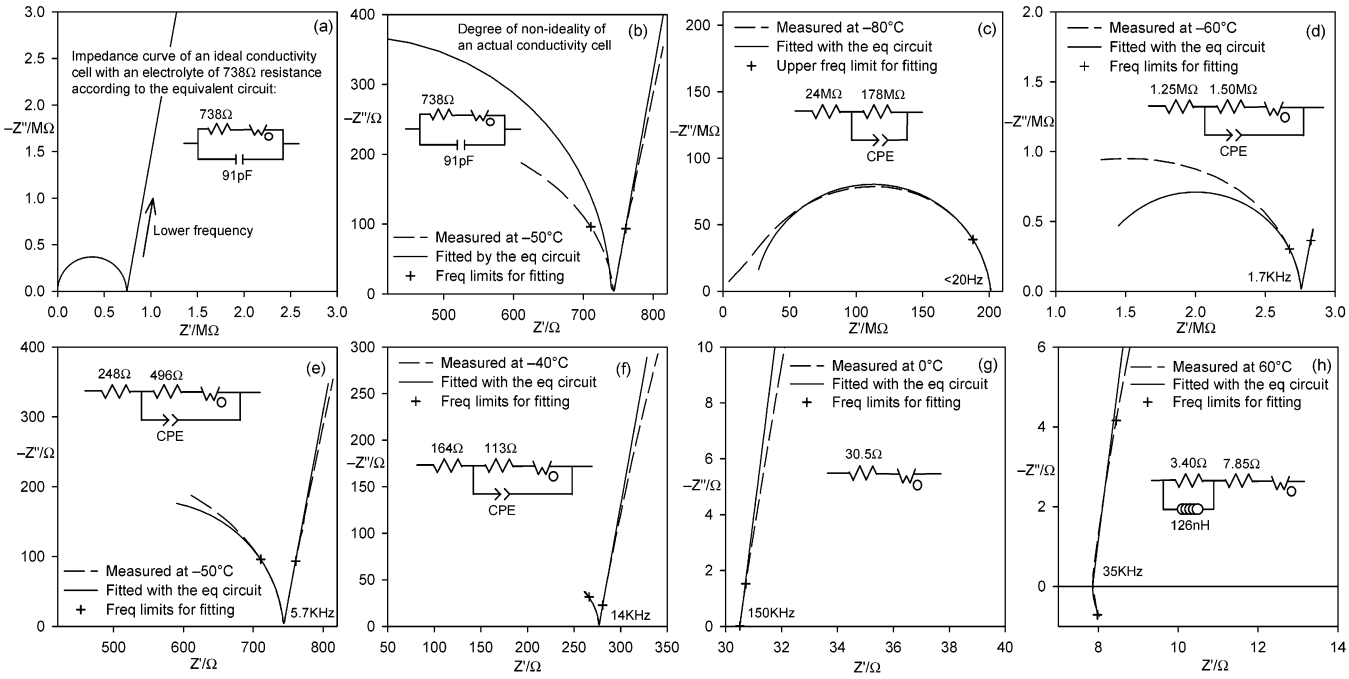

Figure 1. An equivalent circuit for an electrolyte of 738 Ω resistance in an ideal conductivity cell and its simulated impedance curve (a), its fit (solid line) to a measured impedance curve (dashed line) (b), and six sets of measured impedance curves (dashed line), fitted impedance curves (solid line), and the equivalent circuits that generated the fitted curves, for the electrolyte $LiPF_6$(0.89 m) + 0.8PC + 0.2DEC at temperatures of −80, −60, −50, −40, 0, and 60 °C, respectively, from (c) to (h).

ranges of m and w. It is last to show the evaluation results for the vanishing mobility temperature[33] (T_0) and the apparent activation energy (E_a) as appear in the Vogel−Fulcher−Tammann (VFT) equation[34] from fitting the equation to the experimental $\kappa-T$ data and to compare the results with those of T_g.

Experimental Section

Sample Preparation. PC of 99.98% purity and DEC of 99.95% purity were purchased from Grant Chemical, and $LiPF_6$ of 99.9% purity from Stella Chemifa. In an argon-filled drybox, PC and DEC were mixed to form seven mixtures, in addition to pure PC, in mass fractions w of DEC from 0.1 to 0.7 in 0.1 increments, from which eight electrolytes were subsequently made by dissolving $LiPF_6$ into each of the solvents to a molality m of around 2.4 mol kg^{-1}. Conductivity measurement on these solutions and their subsequent dilution for the next set of less concentrated solutions were done in a dry room. At the end of each measurement, a small amount of sample was taken from each electrolyte for the determination of its glass transition temperature.[6]

Measurement of Electrolytic Conductivity. Conductivity κ of the electrolytes was measured with an HP (now Agilent) 4284A precision LCR meter at selected temperatures within a Tenney Jr. Environmental Chamber, controlled and coordinated with a house-made computer program.[6,21] The conductivity cells consisted of a pair of platinum−iridium electrodes and a Pyrex cell body that could be sealed with a ground-glass stopper. The cell constants of a nominal value of 0.1 cm^{-1} were calibrated with a standard KCl solution. The temperature θ of the measurements went from (60 to −80) °C in 10 K decrements, stopping at each for an hour of thermal equilibration before a measurement. The measurement consisted of an impedance scan from 1 MHz to 20 Hz with an amplitude of 10 mV, from which a $Z'Z''$-plot was made and κ was evaluated from the impedance curve in ways to be described in the next section. The precision of the measurement was determined to be 0.04% from 32 replicate measurements on the standard solution at 15 °C under actual measurement conditions. Uncertainty of the measurement was considered for three sources: weighing error in sample preparation, temperature variation of the cell constants, and uncertainty in the sample temperature during measurement. The weighing error uncertainty was estimated to be no more than 0.02% after taking into account the cumulative effect of the successive sample dilutions. Errors due to the temperature variation of the cell constants were estimated to be less than 0.2% in κ. The actual temperatures of the samples during a measurement were recorded with a set of five thermocouples placed next to the sample cells, which were found to stabilize at a temperature slightly off the set temperature, with a temporal distribution of 0.05 K and a spatial distribution of 0.2 K. The error in κ due to these temperature distributions was estimated to be no more than 0.3%. The overall uncertainty in the measurement of κ was therefore estimated to be 0.5%, which should be considered the upper limit of error in every measured value of κ in this work.

Evaluation of Electrolyte Resistance from an Impedance Curve. Due to the varied chemical compositions of the subject electrolytes and the wide temperature range and the limited frequency range within which the electrolytes were measured for their impedance, the measured impedance curves assumed vastly different shapes and their processing to evaluate the electrolyte resistance therefore necessitated the use of different equivalent circuit models and different procedures. The kinds of impedance curves in $Z'Z''$-coordinates commonly encountered are demonstrated in Figure 1c−h with the measured impedance curves of the electrolyte LiPF6(0.89 m) + 0.8PC + 0.2DEC at (−80, −60, −50, −40, 0, and 60) °C, respectively.

It has been proposed[35,36] that the impedance of an electrolyte in an ideal conductivity cell can be modeled with an equivalent circuit of which an example has been depicted in Figure 1a, where the circuit element W_O is the open-circuit Warburg impedance.[37] According to this model,

an electrolyte of 738 Ω would generate in an extended frequency range an impedance curve similar to that plotted in Figure 1a. Conversely, if such an impedance curve is measured for an electrolyte, the electrolytic resistance can be evaluated on the Z'-axis at the point of intersection the semicircle of higher frequencies makes with the long tail of lower frequencies. So, to just evaluate the electrolytic conductivity of an electrolyte from its impedance curve, one only needs to locate this intersection point and develop a reasonable model that fits the curve well near this point. Since direct application of the ideal circuit of Figure 1a did not usually lead to such a good fit, as demonstrated in Figure 1b, the circuit was relaxed in two ways before being used in fitting the impedance curves of the subject electrolytes. The first relaxation was to stop forcing the impedance curve to approach the origin of the $Z'Z''$-plot at high frequencies by inserting a resistor into the circuit, the electrolytic resistance being now the sum of the inserted resistor and the original one. The second was to replace the ideal capacitor with a constant phase element (CPE)[37] to take into account the nonidealities of the actual conductivity cells. The results are the equivalent circuits of Figure 1d−f, where a measured impedance curve consists of a section of a semicircle and a tail section, the length of the former shortening and the latter lengthening with rising temperature. Comparison of a measured curve (dashed line) with a simulated curve (solid line) of the equivalent circuit that has been fitted to the measured one around the intersection point in a range of about four decades in frequency (the limits marked with the crosses) shows a close fit near the intersection point. In fact, the sum of the two resistors of the circuit never differed by more than 0.02% from the Z'-value of the intersection point on the measured impedance curve; the latter was therefore used in these cases as the electrolyte resistance because of its relative ease of computation. At still lower temperatures where an electrolyte becomes very resistive, such as shown in Figure 1c, the tail section does not develop at frequencies higher than the lower frequency limit of the measurement, or, in more severe cases, the low-frequency end of the semicircle terminates some distance away from the Z'-axis. In these cases, the circuit model of Figure 1c, which is that of Figure 1d minus W_O, was found to be appropriate, and the electrolyte resistance was identified with the sum of the resistors in the circuit model that had been fitted to the measured impedance points about two decades in frequency above the end-point frequency. At higher temperatures, on the other hand, the semicircle section does not form below the upper frequency limit, as shown in Figure 1g, and the impedance curve is well fitted by the circuit model of Figure 1g, which is that of Figure 1d minus CPE. For still higher temperatures, there often develops at high frequencies a section of impedance curve with positive Z''-values, as shown in Figure 1h, which can be well fitted with the circuit model of Figure 1h, which is that of Figure 1g plus an inductor and a resistor in parallel. For the last two cases, the Z'-value of the measured impedance point with the smallest Z'-value above the Z'-axis (the peak point) never differed by more than 0.03% from the value of the resistor in the circuit that had been fitted to the measured data points two decades in frequency on one side (or on both sides when available) of the peak point and was therefore used to evaluate the electrolyte resistance for its computational ease. For these cases, replacement of W_O by a CPE and a resistor in parallel resulted in even better fits near the peak point. As the errors involved in the resistance evaluation from the impedance curves were small relative to the other error sources, they were ignored in the overall error analysis.

Finally, it is important to point out that the frequency at which the intersection point or peak point occurs on a measured impedance curve, from which the resistance of the electrolyte is most appropriately evaluated as demonstrated above, varies greatly with the temperature or with the sample resistance, as indicated by the frequency numbers marked near these points in Figure 1c−h. Therefore, significant errors should usually be expected when the conductivity of an electrolyte is determined at a fixed frequency.

Measurement of Glass Transition Temperature. A modulated differential scanning calorimeter (MDSC 2920, TA Instruments) cooled with liquid nitrogen was used to determine the glass transition temperature T_g of a sample. Its temperature scale was calibrated with hexane of 99+% purity (melting point, 177.84 K) and decane of 99+% purity (243.51 K). Vitrification of the sample was achieved by dipping into liquid nitrogen a small amount of sample crimp-sealed in a pair of aluminum pan and lid (0219-0062, Perkin-Elmer Instruments). The sample was then quickly placed onto the DSC sample stage that had been kept at a temperature below T_g of the sample. A modulated heating schedule was then applied, with a heating rate of 2 K min^{-1} and a modulation of 60 s period and 0.5 K amplitude. T_g of the sample was subsequently determined on the reversing component of the heat flow at the inflection point of the endothermic step associated with the glass transition.[6]

Results and Discussion

As will be shown, change of κ of the electrolyte system $LiPF_6(m) + (1 - w)PC + wDEC$ with the m, w, and θ can be consistently explained with changes of ϵ of the solvent and η of the solvent and the solution with the same variables. Thus, ϵ and η of the $PC_{1-w}DEC_w$ binary solvent have been systematically studied, and both were found to fall monotonically and smoothly with w and with θ.[5] This is exactly what one would expect knowing the values of the end-members [the ϵ values of PC and DEC at 40 °C are 61.43 and 2.809, and the η values are (1.91 and 0.622) mPa s, respectively.[20]] and the normal ways ϵ and η of a binary solvent of similar components change with their relative proportions and with θ.[3−11]

Change of Conductivity with Salt Content, Solvent Composition, and Temperature. Results of the κ measurement in the range of (−80, 60) °C for the $LiPF_6(m) + (1 - w)PC + wDEC$ electrolyte are tabulated in Table 1, of which the part from (60 to −40) °C is also plotted in Figure 2 as eight $\kappa-m$ plots with the open circles representing the measured data and the curves plotting their fitting functions $\kappa = f(m,w)$ at the particular temperatures. These functions were obtained by extending the Casteel−Amis equation[31] to include w as an additional variable by setting the equation parameters to polynomial functions of w. That is,

$$\kappa = m^a \exp(b + cm + dm^2) \quad (1)$$

where a, b, c, and d are third-degree polynomials of w:

$$p = p_0 + p_1 w + p_2 w^2 + p_3 w^3 \quad (2)$$

with p standing for a, b, c, or d. Use of eq 1 as the basic form for the fitting functions was due to its ability to faithfully describe the dependency of κ on m in wide ranges of m as shown in Figure 2 and in many other studies,[13,20,23,24,38] which was difficult to achieve with a poly-

Table 1. Measured Values of Electrolytic Conductivity κ (mS cm^{-1}) of the $LiPF_6(m) + (1 - w)PC + wDEC$ Electrolyte at Different Molalities m (mol kg^{-1}), Mass Fractions w, and Temperatures θ (°C) and of Glass Transition Temperatures T_g (K) at the Same Values of m and w

		κ at the following θ														
m	T_g	59.0	49.2	39.3	29.4	19.5	9.7	−0.2	−10.0	−19.8	−29.5	−39.4	−49.3	−59.2	−69.0	−79.0
								$w = 0.0000$								
2.3241	211.8	5.278	3.833	2.608	1.647	0.9521	0.4782	0.1992	0.06444	0.01503	0.002207	0.0001602				
2.1256	207.2	6.288	4.674	3.288	2.167	1.314	0.7061	0.3240	0.1197	0.03297	0.006131	0.0006667	2.978×10^{-5}			
1.9123	201.1	7.365	5.673	4.136	2.824	1.790	1.036	0.5173	0.2146	0.07108	0.01725	0.002594	0.0002043	5.731×10^{-6}		
1.6827	194.7	8.679	6.815	5.142	3.681	2.482	1.542	0.8500	0.4036	0.1570	0.04731	0.009964	0.001211	7.289×10^{-5}	1.252×10^{-6}	
1.4450	188.3	10.05	8.127	6.326	4.717	3.315	2.158	1.288	0.6807	0.3058	0.1123	0.03048	0.005367	0.0005148	2.025×10^{-5}	
1.2341	183.0	11.25	9.225	7.352	5.648	4.150	2.869	1.828	1.052	0.5279	0.2213	0.0714	0.01560	0.002039	0.0001276	2.410×10^{-6}
1.0609	179.3	11.95	9.959	8.079	6.339	4.791	3.425	2.286	1.395	0.7551	0.3500	0.1281	0.03374	0.005590	0.0004771	1.556×10^{-5}
0.9089	175.9	12.29	10.37	8.524	6.799	5.244	3.850	2.656	1.693	0.9691	0.4831	0.1962	0.05888	0.01163	0.001253	5.715×10^{-5}
0.7799	173.7	12.27	10.44	8.661	6.995	5.473	4.094	2.894	1.902	1.134	0.5982	0.2618	0.08669	0.01944	0.002466	0.0001390
0.6659	171.6	11.96	10.24	8.565	6.979	5.533	4.201	3.024	2.039	1.258	0.6930	0.3204	0.1151	0.02865	0.004156	0.0002821
0.5661	169.8	11.41	9.816	8.263	6.786	5.429	4.170	3.049	2.095	1.326	0.7547	0.3650	0.1390	0.03783	0.006117	0.0004755
0.4759	168.2	10.67	9.227	7.803	6.452	5.203	4.038	2.991	2.086	1.351	0.7914	0.3985	0.1602	0.04691	0.008352	0.0007332
0.3958	166.5	9.766	8.470	7.197	5.981	4.855	3.798	2.842	2.013	1.325	0.7947	0.4106	0.1736	0.05390	0.01043	0.001010
0.2801	164.7	7.990	6.954	5.940	4.972	4.070	3.221	2.443	1.761	1.188	0.7341	0.3979	0.1775	0.05974	0.01284	0.001456
0.0000	160.5															
								$w = 0.1000$								
2.3225	208.5	5.758	4.271	2.991	1.953	1.178	0.6269	0.2803	0.09998	0.02636	0.004503	0.0004067	1.357×10^{-5}			
2.1311	204.4	6.802	5.158	3.721	2.523	1.591	0.8976	0.4383	0.1758	0.05382	0.01140	0.001473	8.326×10^{-5}			
1.9117	198.0	7.858	6.117	4.548	3.197	2.114	1.263	0.6660	0.2977	0.1055	0.02811	0.004770	0.0004368	1.632×10^{-5}		
1.6929	191.6	9.257	7.367	5.649	4.123	2.849	1.824	1.045	0.5217	0.2167	0.07096	0.01662	0.002312	0.0001668	4.390×10^{-6}	
1.4535	184.9	10.62	8.686	6.850	5.190	3.717	2.485	1.531	0.8436	0.4004	0.1580	0.04729	0.009424	0.001065	5.304×10^{-5}	
1.2271	180.4	11.89	9.855	7.956	6.209	4.645	3.290	2.158	1.294	0.6847	0.3078	0.1092	0.02733	0.00427	0.0003408	9.729×10^{-6}
1.0532	176.8	12.58	10.58	8.673	6.896	5.295	3.864	2.647	1.671	0.9471	0.4667	0.1865	0.05555	0.01088	0.001173	5.322×10^{-5}
0.8954	173.1	12.86	10.93	9.080	7.332	5.741	4.293	3.032	1.994	1.190	0.6278	0.2765	0.09317	0.02172	0.002951	0.0001843
0.7652	170.7	12.76	10.93	9.157	7.477	5.927	4.510	3.259	2.204	1.364	0.7573	0.3567	0.1315	0.03448	0.005483	0.0004222
0.6524	168.2	12.37	10.66	8.994	7.404	5.939	4.580	3.363	2.325	1.484	0.8560	0.4233	0.1677	0.04837	0.008714	0.0007996
0.5499	166.2	11.72	10.15	8.611	7.138	5.775	4.502	3.353	2.359	1.542	0.9161	0.4724	0.1976	0.06185	0.01236	0.001296
0.4603	164.7	10.90	9.478	8.074	6.735	5.488	4.318	3.254	2.320	1.546	0.9434	0.5035	0.2212	0.07388	0.01612	0.001899
0.3839	163.1	9.947	8.672	7.420	6.217	5.095	4.036	3.068	2.218	1.499	0.9321	0.5092	0.2330	0.08187	0.01915	0.002468
0.3086	162.4	8.779	7.669	6.582	5.539	4.563	3.641	2.790	2.036	1.397	0.8847	0.4970	0.2343	0.08629	0.02148	0.003056
0.0000	158.1															
								$w = 0.1998$								
2.3728	206.6	6.000	4.519	3.232	2.166	1.348	0.7502	0.3551	0.1366	0.03951	0.007546					
2.1648	201.4	7.222	5.569	4.106	2.859	1.863	1.097	0.5658	0.2436	0.08189	0.01947	0.002896	0.0001969	4.697×10^{-6}		
1.9482	195.8	8.241	6.502	4.918	3.536	2.400	1.485	0.8162	0.3851	0.1460	0.04228	0.007944	0.0008212	3.649×10^{-5}		
1.7321	189.4	9.604	7.729	6.008	4.463	3.151	2.070	1.227	0.6384	0.2794	0.09744	0.02472	0.003790	0.0003102	9.656×10^{-6}	
1.4764	183.2	11.08	9.167	7.327	5.643	4.117	2.826	1.796	1.030	0.5140	0.2159	0.07044	0.01572	0.002047	0.0001249	
1.2444	177.9	12.37	10.35	8.462	6.692	5.094	3.683	2.482	1.538	0.8499	0.4034	0.1545	0.04314	0.007809	0.0007546	
1.0529	173.4	13.09	11.12	9.226	7.441	5.809	4.326	3.041	1.984	1.174	0.6113	0.2648	0.08791	0.02006	0.002665	0.0001608
0.8911	169.7	13.31	11.42	9.587	7.843	6.232	4.747	3.430	2.325	1.441	0.7997	0.3780	0.1407	0.03797	0.006308	0.0005201
0.7537	166.9	13.13	11.35	9.606	7.940	6.384	4.944	3.652	2.539	1.630	0.9483	0.4770	0.1932	0.05838	0.01134	0.001153
0.6385	164.6	12.66	10.99	9.367	7.800	6.340	4.969	3.726	2.643	1.744	1.051	0.5531	0.2392	0.07876	0.01720	0.002067
0.5380	163.0	11.93	10.41	8.918	7.472	6.121	4.842	3.675	2.648	1.783	1.102	0.6013	0.2734	0.09636	0.02306	0.003132
0.4496	161.6	11.05	9.682	8.321	7.009	5.777	4.609	3.533	2.576	1.764	1.117	0.6275	0.2975	0.1111	0.02873	0.004347
0.3704	160.7	9.996	8.773	7.569	6.403	5.304	4.259	3.292	2.433	1.687	1.086	0.6248	0.3066	0.1198	0.03310	0.005459
0.2848	158.4	8.548	7.521	6.509	5.531	4.606	3.724	2.903	2.164	1.524	1.000	0.5902	0.2991	0.1226	0.03604	0.006554
0.0000	154.6															

$w = 0.3001$

2.3118	201.8	6.665	5.148	3.815	2.654	1.740	1.035	0.5375	0.2331	0.07911	0.01880	0.002682	0.0001756		
2.1265	197.2	7.685	6.043	4.568	3.283	2.223	1.380	0.762	0.3591	0.1361	0.03819	0.007027	0.0006462	2.387×10^{-5}	
1.9194	191.5	8.784	7.099	5.501	4.058	2.827	1.843	1.077	0.5472	0.2346	0.07871	0.01805	0.002464	0.0001570	3.196×10^{-6}
1.7059	185.4	10.03	8.175	6.505	4.972	3.561	2.448	1.522	0.8230	0.4062	0.1584	0.04653	0.008752	0.0009393	4.352×10^{-5}
1.4664	179.9	11.38	9.532	7.731	6.059	4.519	3.193	2.102	1.244	0.6679	0.3039	0.1100	0.02842	0.004494	0.0003630
1.2514	175.2	12.49	10.42	8.727	6.998	5.427	3.947	2.713	1.722	0.9986	0.5086	0.2110	0.06563	0.01380	0.001654
1.0685	169.7	13.11	11.23	9.406	7.673	6.069	4.617	3.289	2.198	1.343	0.7309	0.3373	0.1219	0.03154	0.005038
0.9088	166.5	13.28	11.49	9.730	8.086	6.454	4.972	3.659	2.528	1.614	0.9277	0.4625	0.1852	0.05592	0.01097
0.7784	163.9	13.07	11.35	9.739	8.103	6.669	5.220	3.857	2.733	1.817	1.076	0.5657	0.2445	0.08129	0.01830
0.6653	162.0	12.71	11.04	9.521	7.844	6.537	5.188	3.936	2.835	1.911	1.181	0.6469	0.2963	0.1065	0.02665
0.5658	160.5	12.00	10.44	9.048	7.516	6.304	5.067	3.836	2.830	1.940	1.235	0.6993	0.3357	0.1279	0.03483
0.4802	158.1	11.28	9.947	8.535	7.281	6.045	4.841	3.751	2.783	1.929	1.257	0.7291	0.3627	0.1452	0.04240
0.3992	157.0	10.18	9.086	7.884	6.711	5.596	4.475	3.543	2.645	1.861	1.230	0.7303	0.3742	0.1568	0.04862
0.3020	155.5	8.781	7.710	6.761	5.78	4.841	3.904	3.118	2.352	1.689	1.133	0.6885	0.3665	0.1611	0.05323
0.0000	151.4														

$w = 0.4001$

2.3304	198.3	6.904	5.417	4.082	2.930	1.986	1.233	0.6817	0.3213	0.1213	0.03350	0.005844	0.0005079	1.576×10^{-5}	
2.1375	194.8	7.943	6.345	4.895	3.608	2.524	1.632	0.9517	0.4825	0.2013	0.06456	0.01409	0.001649	8.350×10^{-5}	
1.9367	189.1	8.923	7.274	5.726	4.329	3.119	2.097	1.281	0.6919	0.3163	0.1158	0.03023	0.004805	0.0003817	1.050×10^{-5}
1.7328	183.3	10.12	8.375	6.731	5.212	3.868	2.710	1.745	1.014	0.5115	0.2145	0.06932	0.01485	0.001882	0.0001085
1.5041	177.7	11.29	9.542	7.826	6.216	4.711	3.398	2.295	1.423	0.7858	0.3750	0.1450	0.04118	0.007415	0.0007101
1.2952	172.2	12.32	10.49	8.753	7.087	5.552	4.154	2.930	1.919	1.140	0.5940	0.2592	0.08708	0.02033	0.002826
1.1019	167.3	12.95	11.17	9.437	7.772	6.221	4.772	3.480	2.379	1.496	0.8436	0.4097	0.1586	0.04559	0.008491
0.9351	164.3	13.13	11.43	9.747	8.128	6.598	5.163	3.855	2.723	1.781	1.061	0.5530	0.2377	0.07891	0.01786
0.7987	161.5	12.96	11.35	9.752	8.200	6.727	5.334	4.056	2.925	1.971	1.220	0.6693	0.3080	0.1126	0.02909
0.6859		12.56	11.04	9.535	8.070	6.679	5.350	4.119	3.022	2.081	1.326	0.7549	0.3664	0.1435	0.04076
0.5857	158.1	11.95	10.54	9.143	7.777	6.478	5.236	4.070	3.028	2.120	1.381	0.8094	0.4096	0.1695	0.05196
0.5023	155.6	11.23	9.949	8.658	7.459	6.191	5.037	3.949	2.967	2.106	1.397	0.8392	0.4383	0.1894	0.06169
0.4233	154.7	10.36	9.187	8.018	6.876	5.781	4.731	3.735	2.834	2.036	1.371	0.8403	0.4507	0.2019	0.06953
0.3256	153.9	8.950	7.960	6.971	6.000	5.074	4.176	3.336	2.548	1.857	1.273	0.7985	0.4424	0.2072	0.07551
0.0000	148.2														

$w = 0.5008$

2.3128	194.7	7.278	5.825	4.499	3.329	2.343	1.528	0.9027	0.4651	0.1983	0.06519	0.01441	0.001756	8.690×10^{-5}	
2.1166	191.2	8.323	6.772	5.350	4.056	2.935	1.990	1.232	0.6774	0.3150	0.1175	0.03149	0.004986	0.0003807	9.341×10^{-6}
1.9198	186.0	9.180	7.612	6.115	4.738	3.518	2.459	1.581	0.9128	0.4576	0.1886	0.05832	0.01174	0.001279	5.501×10^{-5}
1.7117	179.0	10.33	8.681	7.109	5.627	4.290	3.111	2.094	1.287	0.7008	0.3249	0.1204	0.03126	0.005139	0.0004233
1.4766	173.7	11.34	9.719	8.100	6.561	5.093	3.785	2.653	1.725	1.013	0.5236	0.2258	0.07457	0.01670	0.002159
1.2604	167.3	12.20	10.53	8.912	7.339	5.872	4.502	3.277	2.234	1.397	0.7796	0.3731	0.1427	0.04008	0.007244
1.0593	163.9	12.64	11.02	9.443	7.897	6.435	5.048	3.782	2.675	1.760	1.051	0.5530	0.2386	0.08046	0.01886
0.8937	160.1	12.62	11.10	9.580	8.101	6.681	5.329	4.074	2.964	2.014	1.260	0.7022	0.3319	0.1261	0.03476
0.7671	156.3	12.32	10.89	9.460	8.052	6.697	5.398	4.187	3.098	2.155	1.390	0.8072	0.4028	0.1650	0.05040
0.6541	155.4	11.81	10.48	9.140	7.824	6.560	5.335	4.184	3.139	2.227	1.473	0.8830	0.4608	0.2002	0.06639
0.5547		11.12	9.896	8.666	7.45	6.279	5.146	4.070	3.090	2.225	1.500	0.9216	0.4983	0.2268	0.08022
0.4648	151.7	10.28	9.178	8.062	6.957	5.893	4.860	3.875	2.973	2.166	1.486	0.9339	0.5201	0.2464	0.09199
0.3855	149.4	9.337	8.344	7.345	6.360	5.407	4.482	3.597	2.781	2.049	1.424	0.9116	0.5193	0.2536	0.09927
0.2705	147.3	7.538	6.761	5.971	5.190	4.438	3.701	2.997	2.343	1.751	1.239	0.8116	0.4778	0.2439	0.1011
0.0000	144.6														

Table 1 (Continued)

		κ at the following θ													
m	T_g	59.0	49.2	39.3	29.4	19.5	9.7	−0.2	−10.0	−19.8	−29.5	−39.4	−49.3	−59.2	−69.0	−79.0
								$w = 0.5999$								
2.3386		7.294	5.919	4.652	3.517	2.546	1.720	1.066	0.5861	0.2739	0.1027	0.02714	0.004273	0.0003042	6.280×10^{-6}	
2.1490		8.203	6.762	5.421	4.191	3.104	2.172	1.401	0.8141	0.4080	0.1685	0.05190	0.01007	0.001012	3.618×10^{-5}	
1.9321		9.074	7.622	6.220	4.913	3.738	2.691	1.804	1.098	0.5906	0.2675	0.09432	0.02279	0.003172	0.0001945	3.857×10^{-6}
1.7176		10.13	8.619	7.166	5.778	4.504	3.357	2.344	1.509	0.8728	0.4385	0.1812	0.05479	0.01105	0.001210	5.163×10^{-5}
1.4605		11.00	9.539	8.063	6.644	5.267	4.019	2.906	1.969	1.218	0.6719	0.3180	0.1187	0.03186	0.005282	0.0004349
1.2325		11.66	10.18	8.724	7.298	5.949	4.664	3.490	2.465	1.610	0.9530	0.4922	0.2095	0.06864	0.01544	0.001977
1.0464		11.85	10.44	9.045	7.662	6.337	5.062	3.875	2.816	1.915	1.194	0.6652	0.3108	0.1175	0.03249	0.005600
0.8843		11.69	10.38	9.048	7.738	6.467	5.236	4.080	3.035	2.122	1.376	0.8043	0.4063	0.1699	0.05392	0.01148
0.7501		11.28	10.06	8.823	7.593	6.394	5.230	4.129	3.120	2.229	1.487	0.9026	0.4797	0.2144	0.07468	0.01814
0.6372		10.71	9.582	8.434	7.293	6.186	5.099	4.065	3.109	2.262	1.541	0.9614	0.5306	0.2500	0.09344	0.02513
0.5389		9.991	8.966	7.920	6.877	5.860	4.863	3.905	3.017	2.225	1.540	0.9815	0.5589	0.2739	0.1082	0.03131
0.4475		9.137	8.218	7.280	6.343	5.430	4.531	3.664	2.860	2.128	1.499	0.9749	0.5698	0.2894	0.1199	0.03712
0.3622		8.130	7.322	6.500	5.681	4.880	4.093	3.331	2.618	1.970	1.405	0.9304	0.5556	0.2904	0.1255	0.04110
0.2452		6.340	5.731	5.101	4.474	3.863	3.258	2.674	2.123	1.618	1.173	0.7932	0.4882	0.2653	0.1207	0.04249
								$w = 0.7000$								
2.3162		7.372	6.092	4.884	3.789	2.831	1.992	1.303	0.7686	0.3973	0.1711	0.05537	0.01159	0.001240	4.735×10^{-5}	
2.1300		8.139	6.816	5.556	4.403	3.357	2.431	1.647	1.020	0.5580	0.2581	0.09414	0.02330	0.003337	0.0001935	3.045×10^{-6}
1.9264		8.836	7.521	6.235	5.027	3.920	2.908	2.029	1.309	0.7547	0.3762	0.1513	0.04415	0.008137	0.0007348	2.177×10^{-5}
1.7204		9.602	8.262	6.964	5.712	4.545	3.472	2.505	1.682	1.027	0.5547	0.2516	0.08715	0.02105	0.002979	0.0001759
1.4776		10.23	8.948	7.659	6.402	5.182	4.024	2.992	2.092	1.349	0.7887	0.3974	0.1635	0.05016	0.009976	0.001055
1.2541		10.61	9.350	8.100	6.867	5.675	4.532	3.463	2.508	1.692	1.046	0.5701	0.2599	0.09407	0.02429	0.003804
1.0635		10.63	9.443	8.259	7.077	5.927	4.808	3.750	2.789	1.947	1.258	0.7287	0.3638	0.1493	0.04619	0.009510
0.8979		10.32	9.240	8.136	7.027	5.943	4.882	3.866	2.930	2.098	1.401	0.8488	0.4511	0.2022	0.07102	0.01760
0.7640		9.843	8.851	7.830	6.805	5.793	4.798	3.842	2.953	2.152	1.472	0.9224	0.5120	0.2435	0.09275	0.02579
0.6483		9.234	8.333	7.400	6.458	5.534	4.615	3.725	2.897	2.146	1.495	0.9591	0.5517	0.2742	0.1113	0.03398
0.5500		8.551	7.734	6.890	6.036	5.196	4.356	3.541	2.776	2.078	1.471	0.9619	0.5670	0.2927	0.1247	0.04057
0.4612		7.795	7.067	6.311	5.547	4.792	4.038	3.305	2.610	1.974	1.415	0.9428	0.5685	0.3030	0.1343	0.04630
0.3773		6.923	6.291	5.632	4.963	4.302	3.641	2.995	2.384	1.819	1.320	0.8899	0.5492	0.3004	0.1383	0.04995
0.2585		5.407	4.92	4.418	3.908	3.402	2.897	2.401	1.929	1.490	1.098	0.7586	0.4801	0.2718	0.1310	0.05078

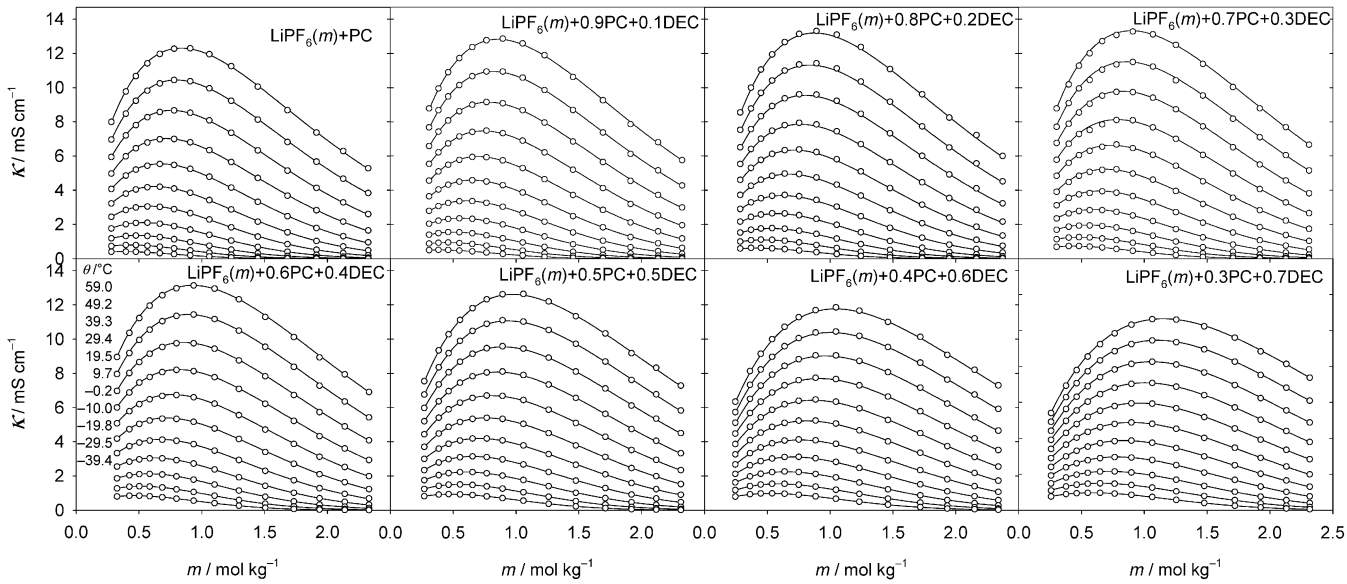

Figure 2. Change of conductivity κ with salt molality m at different temperatures θ and solvent mass fractions w for the $LiPF_6(m) + (1 - w)PC + wDEC$ electrolyte. The open circles represent measured data, and the curves plot their fitting functions of eqs 1 and 2.

nomial function. The choice for the degree of the polynomial of eq 2, on the other hand, was based on its use in eq 1 resulting in the best fit to the measured data. Also, search for an all-inclusive function $\kappa = f(m,w,\theta)$ was attempted by including θ as an additional variable in eq 2 in fitting, resulting in functions that were satisfactory only in limited ranges of the variables. Thus, the bivariate function of eq 1 was fitted to the $\kappa-(m, w)$ data for each θ from (60 to −40) °C for the determination of its parameters, with an average fitting error of 0.63% of the data range. These fitted functions are plotted in Figure 2 with their fitting data to demonstrate the closeness of the fit and in Figure 3 as κ surfaces in mw-coordinates to show the change of κ with simultaneous changes of m and w and with θ.

The κ surfaces as shown in Figure 3 reveal a number of interesting features, the most conspicuous of which is the "dome" shape they assume in the mw-coordinates as a result of κ peaking in both m and w. Peaking of κ in m is a common feature for liquid electrolytes, reflecting the process of κ first increasing with the dissociated ion number as m increases and then falling as the rise of η and of ion association becomes dominant; this has been observed for many electrolytes of lithium salts.[6,13,20−25,31,38] Peaking of κ in w, on the other hand, seems to be the result of the ϵ and η of DEC both being much lower than those of PC and of the mixture both being monotonic functions of w. As such, as w rises from zero, the change of κ is first dominated by the fall of η of the electrolyte causing κ to rise and then by the fall of ϵ of the solvent which by allowing stronger ion association causes κ to fall. The same behavior has been observed in $LiPF_6$ + EC + EMC,[21] where EMC has a much lower ϵ and η than EC, and in $LiClO_4$ + PC + 1,2-dimethoxyethane (DME)[9] and $NaClO_4$ + PC + DME,[10] where DME has a much lower ϵ and η than PC.

Another feature of Figure 3 is the shifting of the κ dome in the direction of low m and high w as θ lowers. This is the result of θ affecting the dome-forming process discussed above. As η rises with lowering θ, the peaking of κ with rising m would occur earlier as the higher η helps to offset the increase in the dissociated ion number. By the same token, the peaking of κ with rising w occurs later as the higher η delays the dominance of ion association over a falling η. The rapid rise of η with falling θ also explains the general fall in height of the domes shown in Figure 3. In addition, as θ lowers, the dome becomes narrower in the direction of m, indicating an increase in the rate with which η rises with m at lower θ. All of these features have been observed in $LiPF_6$ + EC + EMC solution as described in a previous paper.[21]

Change of Glass Transition Temperature with Salt Content and Solvent Composition. Results of the T_g measurement for the $LiPF_6(m) + (1 - w)PC + wDEC$ electrolyte are tabulated in Table 1 and plotted in Figure 4 with the open circles for the measured data and the curves for their fitting function

$$T_g/\mathrm{K} = 160.91 + 11.795m + 6.4786m^2 - 0.91345m^3 - 29.776w - 4.9597w^2 \quad (3)$$

where m is the salt concentration in mol kg^{-1}, w is the mass fraction of DEC, the application range is (0, 2.4) for m and (0, 0.5) for w, and the fitting error is 0.72% of the data range. This equation is also plotted as a T_g surface in the mw-coordinates as the insert in the figure, describing a simple surface slanting down from the corner of high m and low w toward that of low m and high w. This change of T_g, when viewed as a reflection of change in η,[5] is entirely consistent with the change of κ with m, w, and θ as has just been discussed. It also seems that the rise of T_g due to the addition of salt was independent of that due to the change of solvent composition. This can be seen in the shape of the T_g surface and the curves and above all in the absence of a cross-product term in the fitting function of eq 3.

Fitting the VFT Equation to $\kappa-T$ Data. When the $\kappa-T$ data measured for electrolytes of $LiPF_6$ + MOEMC + EC, where MOEMC stands for 2-methoxyethyl methyl carbonate, were fitted with the VFT equation, the vanishing mobility temperature T_0 (also called theoretical glass transition temperature) was found to rise with salt concentration and to differ from T_g by only a few degrees.[26,27] Similarly, for electrolytes of $LiPF_6(m) + (1 - w)EMC + wEC$[21] and $LiPF_6(m) + (1 - w)EC_{0.3}PC_{0.3}EMC_{0.4} + wTFP$,[6] T_0 was found to depend on m and w in the same way as T_g but was lower in value than T_g by a few degrees at the closest approach. One reason for the unusual closeness was suggested to be that the values of T_g of the electrolytes were

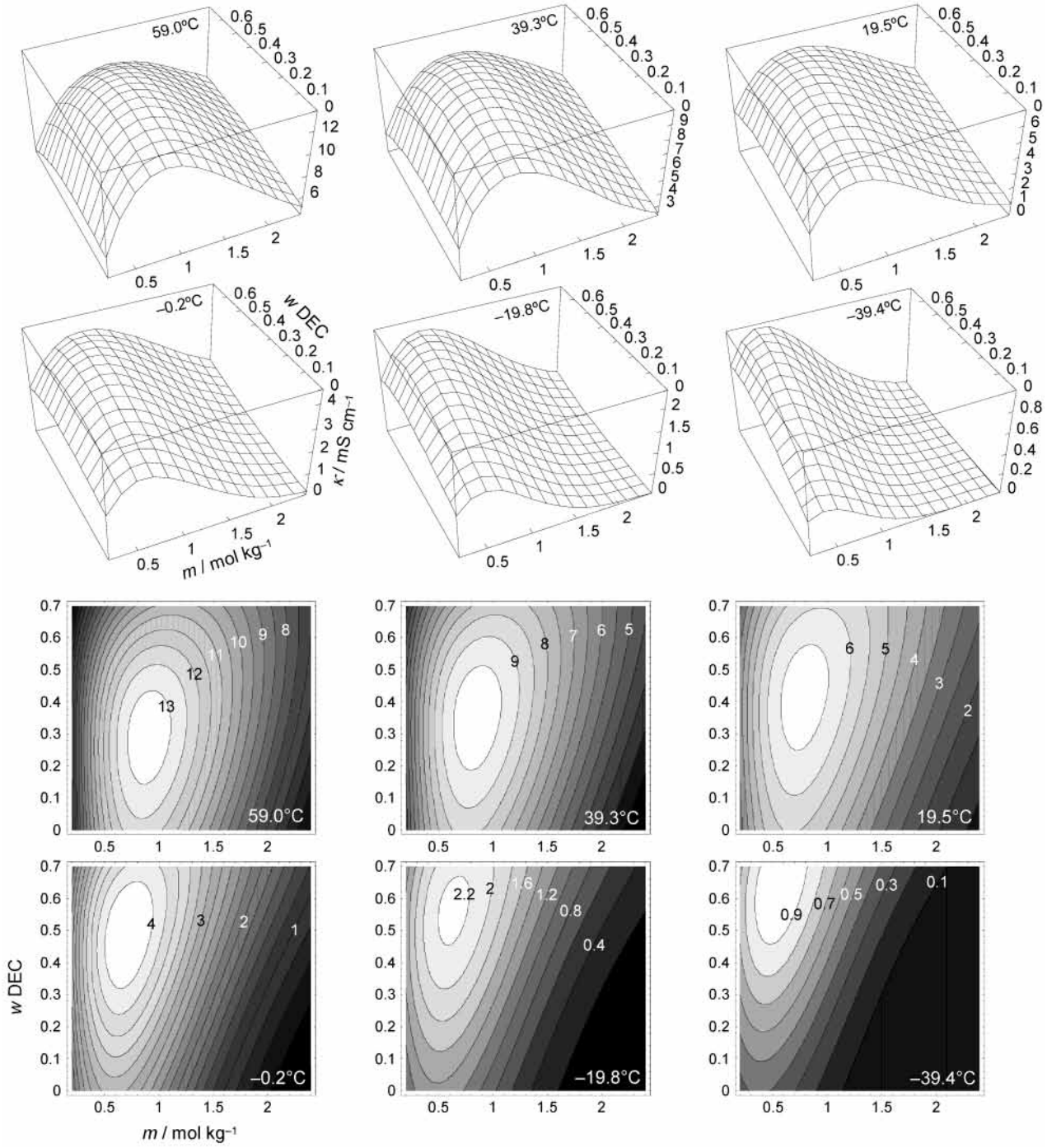

Figure 3. Change of conductivity κ with simultaneous changes in salt molality m and solvent mass fraction w for the $LiPF_6(m) + (1 - w)PC + wDEC$ electrolyte according to eqs 1 and 2 that have been fitted to the $\kappa-(m, w)$ data. Each function is doubly represented by a surface plot (upper plots) and a contour plot (lower plots) with the temperature and the contour values indicated in the plots.

too far below the temperatures at which the fitting data were measured, which were limited to −30 °C by crystallization of EC.[6,21] The $LiPF_6(m) + (1 - w)PC + wDEC$ solution of the present study, being strongly resistant to crystallization, enabled its κ to be measured down to −80 °C, the limit of the temperature control mechanism of the environmental chamber. This limit was on average only 27 K higher than T_g of the samples, the closest being only 10 K. Its $\kappa-T$ data in the range of (−80, 60) °C were therefore fitted with the VFT equation[34]

$$\kappa = \frac{A}{\sqrt{T}} \exp\left(-\frac{E_a}{R}\frac{1}{T - T_0}\right) \qquad (4)$$

where A, E_a, and T_0 are the three fitting parameters with E_a as the apparent activation energy. It was necessary to use the VFT equation in its logarithmic form to fit the ln $\kappa-T$ data in order to avoid fits that would favor data of higher T more strongly than data of lower T, as a result of the much smaller values of κ of the latter than of the former in the wide temperature range. Fitting results of acceptable consistency for T_0 and E_a are shown in Figure 5, with an average fitting error of 0.40% of the data range. An example of the close fit is plotted as an insert in the figure for an electrolyte of $LiPF_6$(0.89 m) + 0.8PC + 0.2DEC, of which the value of κ ranges more than 4 orders of magnitude between (−80 and 60) °C. These fitting values

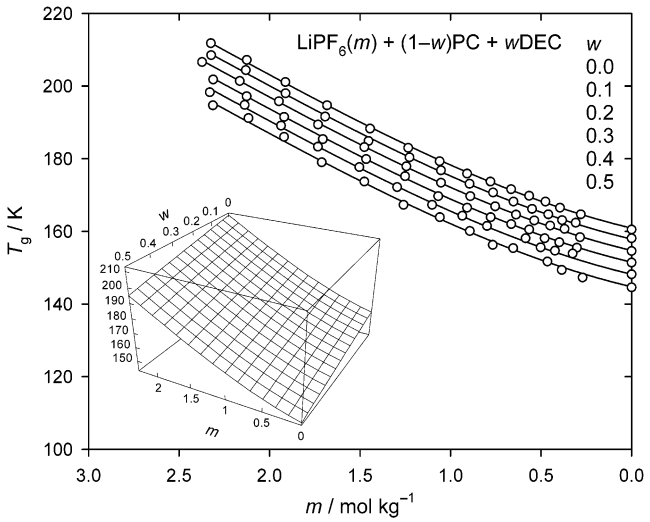

Figure 4. Change of glass transition temperature T_g with salt molality m and solvent mass fraction w for the $LiPF_6(m)$ + (1 − w)PC + wDEC electrolyte. The open circles represent the measured data, and the curves plot their fitting function of eq 3, which is also plotted as a 3D surface as inserted in the figure.

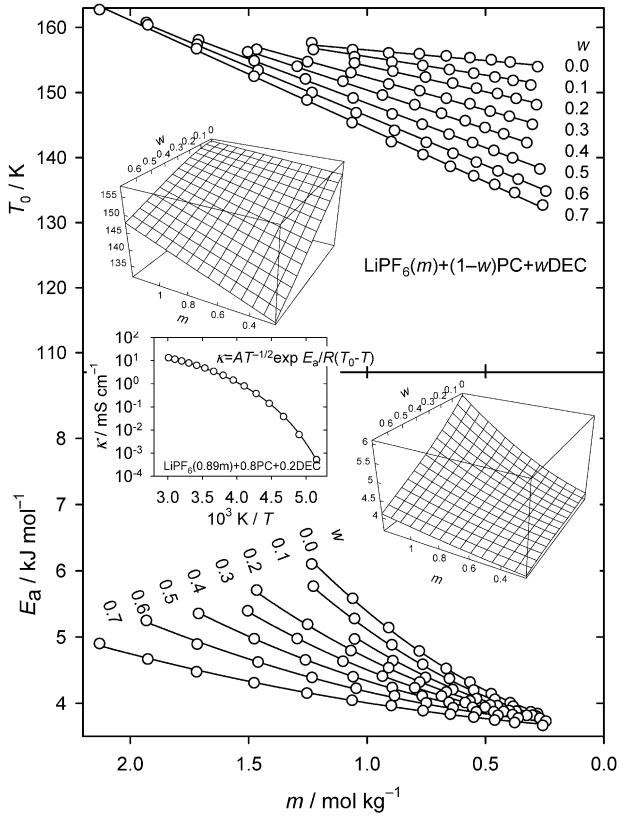

Figure 5. Results of fitting the $\kappa-T$ data with the VFT equation of eq 4 for the $LiPF_6(m)$ + (1 − w)PC + wDEC electrolyte at different salt molalities m and solvent mass fractions w. The upper and the lower plots describe the vanishing mobility temperature T_0 and the apparent activation energy E_a, respectively, with the open circles representing the results from fitting eq 4 and the curves and the surfaces representing the polynomial functions of eqs 5 and 6 obtained from fitting the data of the open circles. The middle insert is an example of the VFT fit to the $\kappa-T$ data of the $LiPF_6$(0.89 m) + 0.8PC + 0.2DEC electrolyte.

as plotted with the open circles in Figure 5 were further fitted with polynomial functions, which are also plotted in the figure with the curves and the 3D surfaces. These polynomials are, for T_0 and E_a in the upper and lower plots,

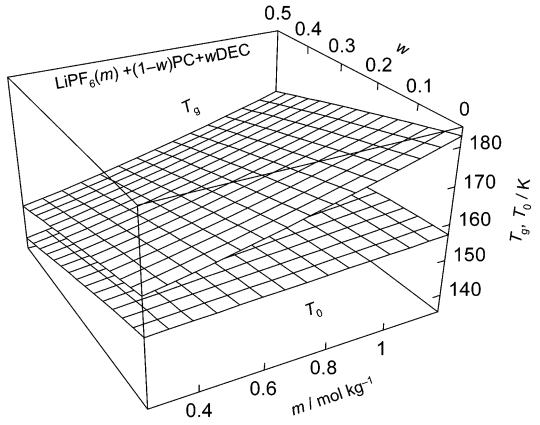

Figure 6. Comparison of T_g and T_0 surfaces as represented by eqs 3 and 5, respectively, in the coordinates of salt molality m and solvent mass fraction w for the $LiPF_6(m)$ + (1 − w)PC + wDEC electrolyte.

respectively,

$$T_0/\mathrm{K} = 153.28 + 3.2633m - 32.937w + 25.181mw - 17.907w^2 - 8.8563mw^2 + 19.107w^3 \quad (5)$$

with the application ranges of (0.25, 1.3) mol kg^{-1} for m and (0, 0.7) mass fraction for w and a fitting error of 0.71% of the data range, and

$$E_a/\mathrm{kJ\ mol^{-1}} = 3.5979 + 0.60061m + 1.1888m^2 + 0.017293w - 1.5114mw - 1.4454m^2w + 1.0792w^2 + 1.3625mw^2 - 1.5177w^3 \quad (6)$$

with the same application ranges and a fitting error of 0.65% of the data range.

The 3D surface of T_0 in the upper plot of Figure 5 shows T_0 to be a simple surface slanting down from the high-η corner of high m and low w to the low-η corner of low m and high w, just like that of T_g shown in Figure 4. This is expected, considering the close connection between T_g and T_0, and has been observed in other electrolyte systems.[6,21] Furthermore, T_0 now lies below T_g with a considerably greater separation than in the other systems,[6,21] as can be seen from Figure 6 where the T_g surface of Figure 4 and the T_0 surface of Figure 5 have been plotted together; the separation is about 30 K at the high-η corner and more than 10 K at the low-η corner. The surface plot for the apparent activation energy E_a, shown in the lower plot of Figure 5, describes another simple surface slanting up from the low-η to the high-η corner, indicating the association of a higher E_a with a higher η. This rise of E_a reflects a rise in the activation barrier to the motion of the ions in the electrolyte, likely as a result of a rising m and a falling w making the electrolyte more viscous. These behaviors of the T_0 and E_a derived here from $\kappa-T$ data, in relation to that of T_g, are entirely consistent with those of the same parameters derived from $\eta-T$ data for many liquids, indicating in the electrolytes of the present study a low degree of decoupling between κ and η or a high degree of assistance provided by the solvent molecules to the ion transport.[26,27] However, some decoupling between κ and η under high-η conditions might still be seen as the cause for the moving away of T_g from T_0 in the direction of high-η shown in Figure 6, given the high reliability of the T_0 values of the present study and the close connection between η of a liquid and its T_g. In addition, judging from the flattening of the E_a surface toward the low-η corner, it

is unlikely that a negative E_a will ever result for an electrolyte of this system, as has been reported for certain low-η electrolytes.[8] For comparison, E_a has been evaluated to range from (4.2 to 4.8) kJ mol^{-1} for some low-η electrolytes[8] and from (5.5 to 9.4) kJ mol^{-1} for some low-melting molten salts.[39]

Conclusions

Electrolytic conductivity κ of the electrolyte system $LiPF_6(m) + (1 - w)PC + wDEC$ was measured and tabulated in the ranges of salt molality m, solvent mass fraction w, and temperature θ of (0.2, 2.4) mol kg^{-1}, (0, 0.7), and (−80, 60) °C, respectively, with an uncertainty of 0.5%. Its glass transition temperature was also measured and tabulated in the same ranges of m and w. The κ in its change with m and w peaked in both variables and thus formed a dome when plotted as a 3D surface in the mw-coordinates, as a result of PC having a dielectric constant ϵ and a viscosity η much higher than those of DEC. In addition, as θ was lowered, the κ surfaces fell in height and shifted in the direction of lower η. The T_g of the electrolyte rose with m and fell with w, the effects of m and w being independent of each other. Fitting a VFT equation to the $\kappa-T$ data measured down to temperatures very close to the T_g resulted in a reliable evaluation of its vanishing mobility temperature T_0 and its apparent activation energy E_a, both forming simple surfaces in the mw-coordinates slanting up in the direction of higher η. Further, the T_0 surface had the same orientation as the T_g surface and was below the latter by more than 10 K.

Literature Cited

(1) Ehrlich, G. M. Lithium-ion batteries. In *Handbook of Batteries*, 3rd ed.; Linden, D., Reddy, T. B., Eds.; McGraw-Hill: New York, 2002.

(2) Hossain, S. Rechargeable lithium batteries (ambient temperature). In *Handbook of Batteries*, 2nd ed.; Linden, D., Ed.; McGraw-Hill: New York, 1995.

(3) *Electrolyte Data Collection. Part 2a. Dielectric Properties of Nonaqueous Electrolyte Solutions*; Barthel, J., Buchner, R., Munsterer, M., Eds.; Chemistry Data Series, Vol. XII; DECHEMA: Frankfurt, 1996.

(4) Barthel, J.; Neueder, R.; Roch, H. Density, Relative Permittivity, and Viscosity of Propylene Carbonate + Dimethoxyethane Mixtures from 25 °C to 125 °C. *J. Chem. Eng. Data* **2000**, *45*, 1007−1011.

(5) Ding, M. S. Liquid-Phase Boundaries, Dielectric Constant, and Viscosity of PC-DEC and PC-EC Binary Carbonates. *J. Electrochem. Soc.* **2003**, *150*, A455−A462.

(6) Ding, M. S.; Xu, K.; Jow, T. R. Effects of Tris(2,2,2-trifluoroethyl) Phosphate as a Flame-Retarding Cosolvent on Physicochemical Properties of Electrolytes of $LiPF_6$ in EC−PC−EMC of 3:3:4 Weight Ratios. *J. Electrochem. Soc.* **2002**, *149*, A1489−1498.

(7) Blomgren, G. E. Properties, Structure and Conductivity of Organic and Inorganic Electrolytes for Lithium Battery Systems. In *Lithium Batteries*; Gabano, J.-P., Ed.; Academic Press: London, 1983.

(8) Matsuda, Y.; Morita, M.; Yamashita, T. Conductivity of the $LiBF_4$/Mixed Ether Electrolytes for Secondary Lithium Cells. *J. Electrochem. Soc.* **1984**, *131*, 2821−2827.

(9) Matsuda, Y.; Morita, M.; Kosaka, K. Conductivity of the Mixed Organic Electrolyte Containing Propylene Carbonate and 1,2-Dimethoxyethane. *J. Electrochem. Soc.* **1983**, *130*, 101−104.

(10) Matsuda, Y.; Satake, H. Mixed Electrolyte Solutions of Propylene Carbonate and Dimethoxyethane for High Energy Density Batteries. *J. Electrochem. Soc.* **1980**, *127*, 877−879.

(11) Payne, R.; Theodorou, I. E. Dielectric Properties and Relaxation in Ethylene Carbonate and Propylene Carbonate. *J. Phys. Chem.* **1972**, *76*, 2892−2900.

(12) *Electrolyte Data Collection. Parts 3a and 3b. Viscosity of Non-Aqueous Solutions II*: *Aprotic and Protic Non-Alcohol Solutions C_1-C_3 and C_4-C_8*; Barthel, J., Neueder, R., Meier, R., Eds.; Chemistry Data Series, Vol. XII; DECHEMA: Frankfurt, 2000.

(13) Cisak, A.; Werblan, L. *High-Energy Nonaqueous Batteries;* Ellis Horwood: New York, 1993; Chapter 7.

(14) Casteel, J. F.; Angel, J. R.; McNeeley, H. B.; Sears, P. G. Conductivity−Viscosity Studies on Some Moderately Concentrated Nonaqueous Electrolyte Solutions from −50° to 125°. *J. Electrochem. Soc.* **1975**, *122*, 321−324.

(15) Petrella, G.; Sacco, A. Viscosity and Conductance Studies in Ethylene Carbonate at 40 °C. *J. Chem. Soc., Faraday Trans. 1* **1978**, *74*, 2070−2076.

(16) Ding, M. S.; Xu, K.; Jow, T. R. Liquid−Solid Phase Diagrams of Binary Carbonates for Lithium Batteries. *J. Electrochem. Soc.* **2000**, *147*, 1688−1694.

(17) Ding, M. S.; Xu, K.; Zhang, S.-S.; Jow, T. R. Liquid/Solid Phase Diagrams of Binary Carbonates for Lithium Batteries, Part II. *J. Electrochem. Soc.* **2001**, *148*, A299−A304.

(18) Ding, M. S. Thermodynamic Analysis of Phase Diagrams of Binary Carbonates Based on a Regular Solution Model. *J. Electrochem. Soc.* **2002**, *149*, A1063−1068.

(19) Ding, M. S.; Xu, K.; Jow, T. R. Phase Diagram of EC-DMC Binary System and Enthalpic Determination of Its Eutectic Composition. *J. Therm. Anal. Calorim.* **2000**, *62*, 177−186.

(20) *Electrolyte Data Collection. Part 1d. Conductivities, Transference Numbers and Limiting Ionic Conductivities of Aprotic, Protophobic Solvents II. Carbonates*; Barthel, J., Neueder, R., Eds.; Chemistry Data Series, Vol. XII; DECHEMA: Frankfurt, 2000.

(21) Ding, M. S.; Xu, K.; Zhang, S. S.; Amine, K.; Henriksen, G. L.; Jow, T. R. Change of Conductivity with Salt Content, Solvent Composition, and Temperature for Electrolytes of $LiPF_6$ in Ethylene Carbonate−Ethyl Methyl Carbonate. *J. Electrochem. Soc.* **2001**, *148*, A1196−A1204.

(22) Barthel, J.; Meier, R.; Conway, B. E. Density, Viscosity, and Specific Conductivity of Trifluoromethanesulfonic Acid Monohydrate from 309.15 K to 408.15 K. *J. Chem. Eng. Data* **1999**, *44*, 155−156.

(23) Barthel, J.; Buestrich, R.; Carl, E.; Gores, H. J. A New Class of Electrochemically and Thermally Stable Lithium Salts for Lithium Battery Electrolytes. II. Conductivity of Lithium Organoborates in Dimethoxyethane and Propylene Carbonate. *J. Electrochem. Soc.* **1996**, *143*, 3565−3571.

(24) Barthel, J.; Gores, H. J.; Schmeer, G. The Temperature Dependence of the Properties of Electrolyte Solutions. III. Conductance of Various Salts at High Concentrations in Propylene Carbonate at Temperatures from −45 °C to +25 °C. *Ber. Bunsen-Ges. Phys. Chem.* **1979**, *83*, 911−920.

(25) Chen, H. P.; Fergus, J. W.; Jang, B. Z. The Effect of Ethylene Carbonate and Salt Concentration on the Conductivity of Propylene Carbonate|Lithium Perchlorate Electrolytes. *J. Electrochem. Soc.* **2000**, *147*, 399−406.

(26) Gu, G. Y.; Bouvier, S.; Wu, C.; Laura, R.; Rzeznik, M.; Abraham, K. M. 2-Methoxyethyl (methyl) carbonate-based electrolytes for lithium batteries. *Electrochim. Acta* **2000**, *45*, 3127−3139.

(27) Gu, G. Y.; Laura, R.; Abraham, K. M. Conductivity−temperature Behavior of Organic Electrolytes. *Electrochem. Solid-State Lett.* **1999**, *2*, 486-489.

(28) Ue, M.; Mori, S. Mobility and Ionic Association of Lithium Salts in a Propylene Carbonate−Ethyl Methyl Carbonate Mixed Solvent. *J. Electrochem. Soc.* **1995**, *142*, 2577−2581.

(29) Ue, M. Mobility and Ionic Association of Lithium and Quaternary Ammonium Salts in Propylene Carbonate and γ-Butyrolactone. *J. Electrochem. Soc.* **1994**, *141*, 3336−3342.

(30) Matsuda, Y.; Nakashima, H.; Morita M.; Takasu, Y. Behavior of Some Ions in Mixed Organic Electrolytes of High Energy Density Batteries. *J. Electrochem. Soc.* **1981**, *128*, 2552−2556.

(31) Casteel, J. F.; Amis, E. S. Specific Conductance of Concentrated Solutions of Magnesium Salts in Water−Ethanol System. *J. Chem. Eng. Data* **1972**, *17*, 55−59.

(32) Ding, M. S.; Jow, T. R. Conductivity and Viscosity of PC−DEC and PC−EC Solutions of $LiPF_6$. *J. Electrochem. Soc.*, in press.

(33) Xu, W.; Angell, C. A. LiBoB and Its Derivatives: Weakly Coordinating Anions, and the Exceptional Conductivity of Their Nonaqueous Solutions. *Electrochem. Solid-State Lett.* **2001**, *4*, E1−E4.

(34) Smedley, S. I. *The Interpretation of Ionic Conductivity in Liquids;* Plenum Press: New York, 1980; Chapter 3.

(35) Feates, F. S.; Ives, D. J. G.; Pryor, J. H. Alternating Current Bridge for Measurement of Electrolytic Conductance. *J. Electrochem. Soc.* **1956**, *103*, 580−585.

(36) Robinson, R. A.; Stokes, R. H. Electrolyte Solutions, 2nd ed.; Butterworth: London, 1959; p 93.

(37) Johnson, D. Help Files for ZView 2.6b; Scribner Associates, Inc.: Southern Pines, NC, 2002.

(38) Choquette, Y.; Brisard, G.; Parent, M.; Brouillette, D.; Perron, G.; Desnoyers, J. E.; Armand, M.; Gravel, D.; Slougui, N. Sulfamides and Glymes as Aprotic Solvents for Lithium Batteries. *J. Electrochem. Soc.* **1998**, *145*, 3500−3507.

(39) McEwen, A. B.; Ngo, H. L.; LeCompte, K.; Goldman, J. L. Electrochemical Properties of Imidazolium Salt Electrolytes for Electrochemical Capacitor Applications. *J. Electrochem. Soc.* **1999**, *146*, 1687−1695.

Received for review December 2, 2002. Accepted March 12, 2003.
JE020219O